Development 133, 1457-1465 (2006) doi:10.1242/dev.02332

Autophagy occurs upstream or parallel to the apoptosome during histolytic cell death

Fatih Akdemir[1], Robert Farkaš[2], Po Chen[1], Gabor Juhasz[3], Lucia Medved'ová[2,4], Miklos Sass[5], Lai Wang[6], Xiaodong Wang[6], Suganthi Chittaranjan[7], Sharon M. Gorski[7], Antony Rodriguez[8] and John M. Abrams[1,*]

Histolysis refers to a widespread disintegration of tissues that is morphologically distinct from apoptosis and often associated with the stimulation of autophagy. Here, we establish that a component of the apoptosome, and pivotal regulator of apoptosis, is also required for histolytic cell death. Using in vivo and ex vivo assays, we demonstrate a global apoptogenic requirement for *dark*, the fly ortholog of Apaf1, and show that a required focus of *dark*$^{-}$ organismal lethality maps to the central nervous system. We further demonstrate that the Dark protein itself is a caspase substrate and find that alterations of this cleavage site produced the first hypermorphic point mutation within the Apaf1/Ced-4 gene family. In a model of 'autophagic cell death', *dark* was essential for histolysis but dispensable for characteristic features of the autophagic program, indicating that the induction of autophagy occurs upstream or parallel to histolytic cell death. These results demonstrate that stimulation of autophagy per se is not a 'killing event' and, at the same time, establish that common effector pathways, regulated by the apoptosome, can underlie morphologically distinct forms of programmed cell death.

KEY WORDS: Autophagy, Apoptosis, *Drosophila*, Histolysis, *dark*

INTRODUCTION

Apical and effector caspases lie at the core of the apoptotic program (Danial and Korsmeyer, 2004). Upon interaction with adaptor molecules, apical caspases are stimulated to activate effector caspases by proteolysis. *dark*, the *Drosophila* homolog of nematode Ced-4 and mammalian Apaf1, is thought to regulate the apical caspase *Dronc* (*Nc* – FlyBase), through interactions involving respective caspase recruitment domains (CARD) (reviewed by Mills et al., 2005). As in mammalian systems, fly caspases are also subject to negative regulation by IAP proteins (Danial and Korsmeyer, 2004), and, among *Drosophila* members of this family, Diap1 (Thread – FlyBase) is known to exert important control over apoptosis (Goyal, 2001; Wang et al., 1999). This protein binds *Dronc* and the effector caspase *Drice* (*Ice* – FlyBase), inhibiting the activity of each via multiple mechanisms (Ditzel et al., 2003; Hays et al., 2002; Martin, 2002; Meier et al., 2000; Ryoo et al., 2002; Wilson et al., 2002; Wing et al., 2002b). Diap1 itself is under tight regulation and is effectively antagonized by proapoptotic proteins [*reaper* (*rpr*), *grim*, *hid* (also known as *Wrinkled*) and *skl*] encoded in the *reaper* region (Chai et al., 2003; Christich et al., 2002; Silke et al., 2004; Wing et al., 2002a; Wing et al., 2002b; Wing et al., 2001; Wu et al., 2001; Yoo et al., 2002; Zachariou et al., 2003). Together, these linked genes specify virtually all programmed cell death (PCD) in the fly embryo, as the combined deletion of these eliminates PCD at this stage (Abrams, 1999).

Three broadly conserved protein families, represented by Ced-9/Bcl2, Ced-4/Apaf1 and Ced-3/Caspase 9, define fundamental components in pathways of caspase control. However, a unified mechanism for their action in cell death remains elusive, as analogous physical interactions seen between nematode Ced-9 and Ced-4 do not occur among orthologous mammalian counterparts (Moriishi et al., 1999). Instead, mammalian Bcl2 proteins indirectly engage Apaf1 by controlling the mitochondrial release of cytochrome c, which promotes the formation of a multimeric complex referred to as the apoptosome (Danial and Korsmeyer, 2004; Spierings et al., 2005). Although the fly counterparts of these genes add provocative clues, particularly with respect to the negative regulators of caspase activity (Salvesen and Abrams, 2004), they also complicate the picture, as cytochrome c appears dispensable for *Drosophila* Apaf1 (*Dark*)-dependent cell death, despite the conservation of a WD domain thought to be necessary for cytochrome c binding and regulation (Adrain et al., 1999; Dorstyn et al., 2004; Hu et al., 1998; Rodriguez et al., 1999; Zimmermann et al., 2002). Previous data from us, and from others, on viable hypomorphic alleles (Kanuka et al., 1999; Rodriguez et al., 1999; Zhou et al., 1999) have established that *Dark* shares functional properties with its counterparts in *C. elegans*, where Ced-4 is required for all PCD, and in the mouse, where context-specific apoptogenic requirements for Apaf1 are seen. However, central questions, approachable only with a null allele, remained open.

Here, we isolate a single-gene null mutation at *dark* and demonstrate a general requirement for this gene in PCD and stress-induced apoptosis. The role for *dark* in PCD was not absolute, however, as rare cell deaths were observed. We show that a required focus of *dark*$^{-}$ organismal lethality maps to the central nervous system and also describe the first hypermorphic allele within the Apaf1/Ced-4 gene family. In a model of tissue histolysis, *dark* was essential for cell death but dispensable for characteristic features of the autophagic program, indicating that the stimulation of autophagy

[1]Department of Cell Biology, UT Southwestern Medical Center, Dallas, TX 75390, USA. [2]Institute of Experimental Endocrinology, Slovak Academy of Sciences, Vlarska 3, 83306 Bratislava–Kramare, Slovakia. [3]Department of Genetics, Cell Biology and Development, University of Minnesota, 6-160 Jackson Hall, 321 Church Street SE, Minneapolis, MN 55455, USA. [4]Department of Genetics, Faculty of Science, Comenius University, 84215 Bratislava, Slovakia. [5]Department of General Zoology, Lorand Eotvos University, Pazmany setany 1/C, H-1117 Budapest, Hungary. [6]Department of Biochemistry, UT Southwestern Medical Center, Dallas, TX 75390, USA. [7]Genome Sciences Centre, BC Cancer Research Centre, 675 West 10th Avenue, Vancouver, BC V5Z 1L3, Canada. [8]Wellcome Trust, Sanger Institute, Genome Campus, Cambridge CB10 1SA, UK.

*Author for correspondence (e-mail: John.Abrams@utsouthwestern.edu)

Accepted 17 February 2006

per se is not the mechanism of cell killing but lies upstream, or parallel to *dark*. These data establish that common effector pathways, regulated by the apoptosome, specify apoptotic and histolytic forms of PCD.

MATERIALS AND METHODS

Mutagenesis

To isolate deletions that eliminate *dark* without compromising the function of adjacent neighboring genes, a P insertion associated with $dark^{CD4}$ (Rodriguez et al., 1999) was remobilized and candidates were tested in trans to existing alleles and against lethal mutations in flanking genes. Promising 'hits' were screened by PCR. $dark^{82}$ failed to complement $dark^{CD4}$, but complements adjacent lethal alleles in the neighboring genes, RhoGEF and a new lethal P mutation in CG8963 that we fortuitously obtained in our first round of mutagenesis. Genomic PCR across the deletion junction and RT-PCR were used to validate the mutation and define the $dark^{82}$ lesion. *yw* was the parental wild-type strain for molecular analysis and for ex vivo hemocyte studies. RNA extraction and QRT-PCR were conducted as described by Gorski et al. (Gorski et al., 2003). Ages at 25°C were normalized from 18°C (Park et al., 1996). Genomic PCR and RT-PCR were performed as described by Chew et al. (Chew et al., 2004), with relevant gene-specific primers.

Transgenic 'rescue' and genetic manipulation

Full-length *dark* with 8×His-tags at the N terminus and 3×Myc-tags at the C terminus was cloned into the *Bam*HI/*Xho*I sites of the pFastBac1 vector (Invitrogen). The *Bam*HI/*Xho*I insert was then subcloned into the pUAST vector to produce pUAST-$dark^{WT}$. pUAST-$dark^{V}$ was generated by changing Aspartate 1292 to Alanine using a QuikChange Site-Directed Mutagenesis Kit (Stratagene). The pUAST constructs were injected into fly embryos following standard procedures to obtain transformants. Independent transgenic lines were mapped and crossed to the $dark^{82}$ background. For rescue experiments, $dark^{82}$*/CyO, actin-GFP;UAS-*$dark^{WT}$ or $dark^{82}$*/CyO, actin-GFP;UAS-*$dark^{V}$ flies were crossed to $dark^{82}$*/CyO, actin-GFP; Tub-Gal4/TM3, Sb* flies (or other drivers). The number of homozygous $dark^{82}$*; UAS-dark/Tub-Gal4* progeny and number of heterozygous $dark^{82}$*/CyO, actin-GFP; UAS-dark/Tub-Gal4* progeny were counted. The percent of rescue was calculated by dividing the number of rescued $dark^{82}$ homozygotes by the Mendelian value expected if $dark^{82}$ homozygotes were fully viable. Similar crosses were used to obtain $dark^{82}$*; UAS-dark/Hml-Gal4* L3 larvae for hemocyte isolation. *c81-Gal4, c833-Gal4* and *Hml-Gal4* strains (Drapeau et al., 2003; Goto et al., 2003; Hrdlicka et al., 2002; Manseau et al., 1997) were obtained from the Bloomington Stock Center.

Germline clones and AO staining

The $dark^{82}$ allele was recombined onto the $FRT^{2R\text{-}G13}$ chromosome. To generate $dark^{82}$ maternal-null embryos, the Dominant Female Sterile (DFS) technique was used, as described previously (Chou and Perrimon, 1996). *hs-Flp/+; OvoD* $FRT^{2R\text{-}G13}$/$dark^{82}$ $FRT^{2R\text{-}G13}$ females were crossed with $dark^{82}$*/CyO, actin-GFP* males to generate maternal and zygotic *dark*-null embryos. To detect cell death, Acridine Orange (AO) staining was carried out (Abrams et al., 1993).

Ex vivo hemocyte analyses

Wandering L3 instar larvae were prepared as described by Chew et al. (Chew et al., 2004), with the following modifications. Hemolymph was collected from six larvae and agents were added after media addition. Membrane blebbing, a characteristic feature of apoptosis, was used to quantify apoptosis. At ~6 hours post-treatment, cells were stained with a fluorescent membrane dye, 10 uM CellTracker (Molecular Probes) in DMSO, to facilitate the visualization of apoptotic membrane blebbing (without fluorescent labeling it was difficult to assess membrane blebbing owing to the phagocytic nature of hemocytes).

Immunohistochemistry and western blotting

Immunohistochemistry on dissected salivary glands was conducted as described by Farkas and Mechler (Farkas and Mechler, 2000). For actin counterstaining, fluorescein-conjugated phalloidin (1:200; Molecular Probes), or AlexaFluor488-Phalloidin or AlexaFluor546-Phalloidin (Molecular Probes) was used; for nuclear counterstaining, 0.5 μg/ml Hoechst 33258 (Calbiochem) or 1 μg/ml OliGreen (Molecular Probes); and for caspase activity, rabbit anti-cleaved caspase-3 antibody (1:500; Cell Signaling Technology). Optical sections (0.5 μm thick) were collected using a Zeiss LSM-510 Meta laser confocal microscope equipped with a 40× planapochromat oil objective. Recombinant Dark protein was prepared as described previously (Yu et al., 2005). Transgenic Dark protein was detected in extracts from adult heads, with an anti-Myc antibody at a dilution of 1:2000. Anti-Dark polyclonal antibody was used at a dilution of 1:3000.

Electron microscopy

Samples were prepared and processed for electron microscopy as described previously (Juhasz and Sass, 2005).

Visualization of MDC and GFP-LC3

Transgenic flies containing UAS-GFP-LC3 were kindly provided by the Harald Stenmark Laboratory (Rusten et al., 2004) and crossed to flies containing the salivary gland driver D59-Gal4 (Gustafson and Boulianne, 1996) (kindly provided by Carl Thummel). Salivary glands of the progeny were dissected in *Drosophila* Schneider's medium (Invitrogen) and transferred to the same medium with MDC (0.1 mM) for 30 minutes at room temperature. Samples were then rinsed once and mounted (both in Schneider's medium). Salivary glands were analyzed by fluorescence microscopy using a Zeiss Axioplan 2 microscope.

RESULTS

$dark^{82}$ is null allele

To investigate the molecular genetic properties of the *Drosophila* apoptosome, and to illuminate possible 'non-death' roles for the *dark* gene in development, we recovered a null mutation at *dark* in a screen for excision derivatives of an existing P insertion (Rodriguez et al., 1999). $dark^{82}$ is a 6.3-kb deletion spanning the entire open-reading frame and nearly the entire transcription unit (Fig. 1A-C). Animals homozygous for this allele arrest as late pupae and often present a characteristic dark blister located centrally along the midline. The mutation fails to complement all existing hypomorphic *dark* alleles, but complements flanking genes (see Materials and

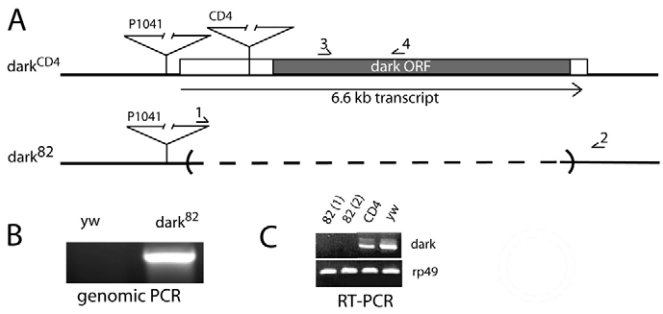

Fig. 1. Generation of a $dark^{82}$ null mutation. (**A**) Schematized view of the genomic structure of the *dark* locus, relevant alleles and the $dark^{82}$ null mutation. The *dark* transcript spans 6.6 kb. $dark^{82}$ is a 6324 bp deletion (dashed line) generated by imprecise excision of the indicated P-element in the $dark^{CD4}$ strain (Rodriguez et al., 1999). The allele was mapped by sequencing a 1.3 kb genomic PCR fragment (see **B**) using a primer pair (designated 1 and 2) spanning the junctional interval. In $dark^{82}$, sequences from –1277 bp (upstream of the translation start codon) to 19 bp downstream of the stop codon are absent such that the entire *dark* ORF and part of the untranslated first exon are missing. Note that 396 bp of sequence from the CD4 transposon remain at this junction. (**C**) RT-PCR with primer pair 3 and 4, using total RNA from prepupae, confirms complete loss of the *dark* transcript in the $dark^{82}$ allele. Two different isolates of $dark^{82}$ from the screen were assayed here, 82 (1) and 82 (2). rp49 is a control.

Table 1. Tissue-specific rescue by wild-type *dark* and a hypermorphic allele

	Driver	Percentage of rescued $dark^{82}$ homozygous flies
UAS-$dark^{WT}$.H4	No	0% (27)
UAS-$dark^{WT}$.B6	No	0% (24)
UAS-$dark^{V}$.C8	No	33% (18)
UAS-$dark^{V}$.G6	No	23% (30)
UAS-$dark^{WT}$.H4	Tubulin-Gal4	100% (27)
UAS-$dark^{WT}$.B6	Tubulin-Gal4	95% (38)
UAS-$dark^{V}$.C8	Tubulin-Gal4	92% (25)
UAS-$dark^{V}$.G6	Tubulin-Gal4	97% (30)
UAS-$dark^{WT}$.H4	Dal-Gal4	100% (34)
UAS-$dark^{WT}$.B6	Dal-Gal4	96% (25)
UAS-$dark^{V}$.C8	Dal-Gal4	103% (35)
UAS-$dark^{V}$.G6	Dal-Gal4	95% (29)
UAS-$dark^{WT}$.H4	Hml-Gal4	0% (22)
UAS-$dark^{WT}$.B6	Hml-Gal4	0% (33)
UAS-$dark^{V}$.C8	Hml-Gal4	29% (35)
UAS-$dark^{V}$.G6	Hml-Gal4	18% (29)
UAS-$dark^{WT}$.H4	pCNS-Gal4 (c81)	16% (62)
UAS-$dark^{WT}$.B6	pCNS-Gal4 (c81)	18% (80)
UAS-$dark^{WT}$.H4	c833-Gal4	0% (23)
UAS-$dark^{WT}$.B6	c833-Gal4	0% (25)

Data from transgenic rescue experiments is summarized. Reversal of $dark^{82}$ lethality was scored in contexts where tissue-specific expression of a wild-type transgene (UAS-$dark^{WT}$) or a *dark* variant transgene (UAS-$dark^{V}$) were tested. The left-hand column indicates the transgene tested in combination with the tissue 'driver' listed in the middle column. In each case, a single dose of the *dark* transgene and driver are tested. The right-hand column indicates the percentage of rescued animals relative to the expected Mendelian value, listed in parentheses. Note that, for each transgene, at least two independent lines were tested (H4 and B6 for UAS-$dark^{WT}$, and C8 and G6 for UAS-$dark^{V}$). $dark^{82}$ lethality is fully rescued if UAS-$dark^{WT}$ is driven by Tubulin-Gal4 or by Dal-Gal4, which both confer ubiquitous expression. By contrast, no rescue is observed if UAS-$dark^{WT}$ is combined with an embryonic CNS/larval disc driver (c833-Gal4) or a hemocyte-specific driver (Hml-Gal4). However, substantial rescue of $dark^{82}$ lethality occurs when expression of UAS-$dark^{WT}$ is restored in the post-embryonic CNS using the pCNS-Gal4 driver, also called c81-Gal4 and expressed diffusely throughout brain lobes, but not in embryos, egg chambers or imaginal discs (Drapeau et al., 2003; Manseau et al., 1997). Surprisingly, in the absence of any Gal4 driver, 'leaky' expression of $dark^{V}$ partially rescued $dark^{82}$ lethality, but wild-type *dark* did not.

methods). Homozygous $dark^{82}$ animals were rescued to viability using a transgene containing a full-length *dark* cDNA (see Table 1). Hence, $dark^{82}$ is a lethal, single-gene null mutation.

Elimination of maternal and zygotic *dark*

Because animals homozygous for $dark^{82}$ survive to pupation, we used the Dominant Female Sterile technique to examine the phenotypes of animals lacking maternally supplied *dark* (see Materials and methods). We found normal PCD patterns in embryos that retained zygotic, but lacked maternal, *dark* (Fig. 2A,B). By contrast, embryos devoid of both maternal and zygotic *dark* were almost entirely cell death defective, with rare cell deaths noticeable in later-staged animals (Fig. 2C,D). These observations demonstrate a global need for *dark* in PCD. However, the requirement is not absolute, as occasional apoptotic cell deaths did occur in the complete absence of *dark* function. Embryos lacking maternal and zygotic *dark* failed to hatch and were also defective for head involution, similar to cell-death defective mutations in the *Reaper* region (Grether et al., 1995; White et al., 1994) and *dronc* (Chew et al., 2004). At the same time, gastrulation, segmental patterning and extension of the germ band appeared grossly normal in the absence of *dark*. Hence, to the extent that these events involve migration and/or movement, we note that the proposed role for *dark* in cell motility evidently does not generalize to these morphogenic processes (Geisbrecht and Montell, 2004). We also tested larval

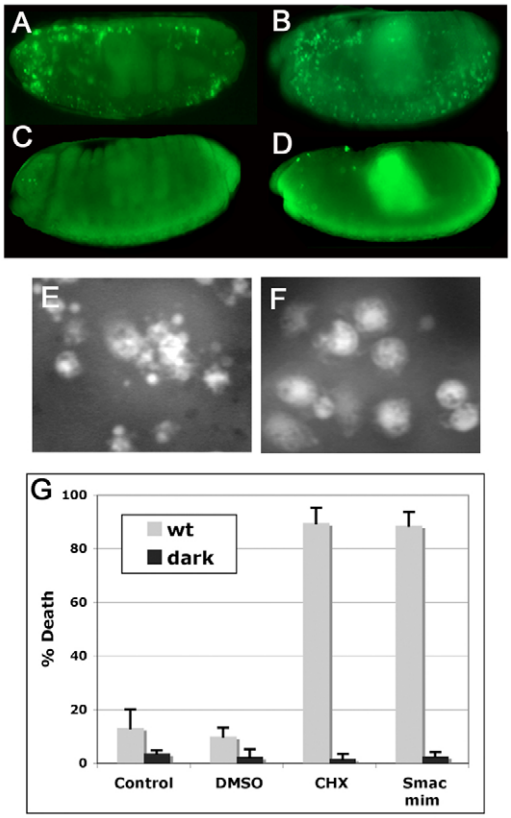

Fig. 2. *dark* is essential for programmed and unprogrammed apoptosis. (**A-D**) Maternal and zygotic sources of *dark* were removed using a Dominant Female Sterile strategy (see Materials and methods). The resulting embryos lacked nearly all PCD, shown here by Acridine Orange (AO) staining (green). A and B show mid-staged embryos eliminated for maternal *dark* but heterozygous for zygotic *dark*; C and D show comparably staged embryos lacking both maternal and zygotic *dark*. Note that without a source of *dark*, embryos are head involution defective with only few AO-positive cells (C,D). (**E-G**) Requirement for *dark* in models of stress-induced cell death. Hemocyte aspirates from $dark^{82}$ and wild-type (wt) wandering third instar larvae were treated with chemical stressors ex vivo and stained with CellTracker (see Materials and methods). Induction of apoptosis in wild-type (E) but not $dark^{82}$ (F) hemocytes is exemplified here with micrographs taken 6 hours after Cycloheximide (CHX) treatment. (G) Quantification of apoptosis 6 hours after challenge with either CHX or a Smac mimetic (Li et al., 2004) are plotted as the incidence of cell death in percentages. Error bars indicate s.d.

hemocytes in ex vivo models of stress-induced cell killing (Fig. 2E-G). In contrast to wild-type counterparts, $dark^{-}$ hemocytes were completely resistant to a Smac mimetic, which antagonizes inhibitor of apoptosis proteins (IAPs) and is thought to simulate the action of *reaper* proteins (Li et al., 2004; Salvesen and Abrams, 2004). Likewise, $dark^{-}$ cells were completely insensitive to the apoptogenic effects of cycloheximide, a protein synthesis inhibitor. Together, these data establish a central role for the action of *dark* in programmed and unprogrammed apoptosis.

Tissue-specific restoration in the CNS reverses $dark^{-}$ lethality

To confirm and extend these studies, we restored *dark* using a transgene (designated UAS-$dark^{WT}$) that places a full-length cDNA under the control of the yeast-derived UAS promoter, which permits

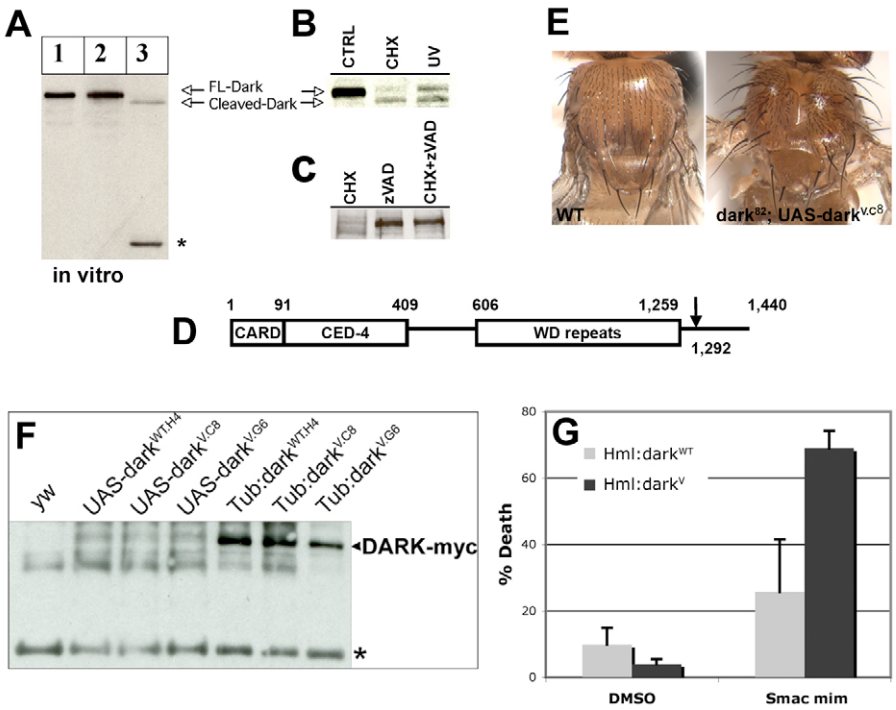

Fig. 3. Alteration of a caspase cleavage site produces a hypermorphic Dark variant. (**A**) Recombinant Dark protein (lane 1) was incubated with cytosolic S20 fractions prepared from control S2 cells (lane 2) or cycloheximide (CHX)-treated S2 cells (lane 3). Asterisk denotes the small Dark C-terminal fragment after cleavage. (**B**) Consistent with in vitro studies (A), stimulus-dependent cleavage of Dark is detected here in *Drosophila* S2 cells. Samples from unchallenged (Ctrl) S2 cells or cells treated with 20 μM Cycloheximide (CHX) or 200 mJ/cm^2 UV were harvested after 4 hours. (**C**) Cleavage of Dark as seen in panel B with CHX treatment, is reversed by the caspase inhibitor z-VAD (100 μM), shown here 5 hours post-treatment. In A,B and C, Dark was visualized with an anti-Dark polyclonal antibody. (**D**) The cleavage site, detected in vitro at residue 1292, is shown (arrow) in the schematized domain structure of the Dark protein. (**E**) Illustration of the defective anatomy of *dark*^{82} flies rescued by leaky expression of UAS-dark^{V}, which mutates the caspase site mapped in D. The notum of a *dark*^{82} homozygote rescued to viability by UAS-dark^{V}, shown here next to a wild-type fly notum (left), exhibits a 'split thorax' phenotype and bristle abnormalities. (**F**) Levels of transgenic Dark protein in various UAS-dark transgenic lines in the absence of any driver or under Tubulin-Gal4 were examined by immunoblot using an anti-Myc antibody. Arrowhead denotes Dark-myc; asterisk indicates an irrelevant cross-reacting band showing equal loading on each lane. Note that the levels of wild-type Dark and Dark^{V} are comparable when expressed from the Tubulin-Gal4 driver or when examined for basal expression. (**G**) Hemocyte aspirates from dark^{82}; Hml-Gal4:UAS-dark^{WT} (Hml:dark^{WT}) and dark^{82}; Hml-Gal4:UAS-dark^{V} (Hml:dark^{V}) L3 larvae were treated with DMSO or the Smac mimetic (Li et al., 2004), a potent apoptotic inducer. Expression of UAS-dark^{WT} in dark^{82} hemocytes only mildly restored apoptosis after Smac mimetic treatment. However, UAS-dark^{V} almost completely restored this apoptotic response to dark^{82} hemocytes.

conditional expression when combined with tissue-specific Gal4-driver strains. Table 1 shows that, in two independently transformed lines, ubiquitous expression of wild-type *dark*, using either Tubulin-Gal4 or Daughterless-Gal4 drivers, completely rescued *dark*^{82} lethality. In parallel studies, the expression of UAS-dark^{WT} in mutant hemocytes (via the Hml-Gal4 driver) did not rescue viability, but did partially restore sensitivity to Smac mimetic killing to these cells (Fig. 3G). Surprisingly, exclusive restoration of *dark* to the post-embryonic central nervous system using pCNS-Gal4 (also called c81-Gal4) reversed *dark*^{82} lethality, but restoration of *dark* to the embryonic CNS and imaginal discs (c833-Gal4 driver) did not. Although we cannot exclude the possibility that maternal *dark* is depleted in the CNS earlier than in other tissues, these results demonstrate that, at minimum, expression of *dark* in the post-embryonic CNS is necessary to reverse organismal lethality and to produce a viable adult. We also note here that male and female adults rescued by pCNS-Gal4 driven *dark* were sterile. However, in DAPI-stained preparations, no associated defects in germ line formation were detected at the gross morphological level.

A caspase cleavage site in Dark confers hypermorphic gene activity when mutated

Exploratory in vitro studies with recombinant Dark identified a putative caspase cleavage site that was mapped to Asp1292 (Fig. 3A,D). Consistent with this, studies using *Drosophila* S2 cells detected a cleavage of Dark that matched predictions from in vitro studies (Fig. 3B) and was caspase dependent, as it was prevented by the caspase inhibitor ZVAD (Fig. 3C). To examine the biological effects of this site in vivo, we tested a variant *dark*^{v} (see Materials and methods) that substitutes Ala for Asp at position 1292. Like wild-type transformants, ubiquitous restoration of this *dark* variant (UAS-dark^{v}) reversed the lethality caused by *dark*^{82} (Table 1). However, in the absence of any Gal4 driver, 'leaky' expression of UAS-dark^{v} also rescued *dark*^{82} lethality but, surprisingly, wild-type *dark* did not (Table 1). Therefore, dark^{v} exhibits hypermorphic gene action relative to wild-type *dark*. In fact, adult flies rescued to viability with *dark*^{v} displayed split thorax phenotypes and bristle abnormalities in the notum (Fig. 3E) that resemble *dark*^{cd4} homozygotes (Rodriguez et al., 1999). Together, these observations indicate that leaky expression of dark^{V} restores gene function to null animals, not to the wild-type level but, instead, to levels comparable to those seen in *dark*^{cd4}. Hypermorphic properties related to dark^{v} were also noted in ex vivo hemocyte assays. Expression of the wild-type cDNA in dark^{82} hemocytes only mildly restored stimulus-dependent apoptosis after treatment with a Smac mimetic. However, dark^{V} almost completely restored this apoptotic response to dark^{82} hemocytes (Fig. 3G). We considered the possibility that altered expression of UAS-dark^{v} might explain the hypermorphic properties conferred by dark^{V} but, as shown in Fig. 3F, the expression levels of wild-type and variant transgenes were equal. Therefore, in studies of organismal viability and hemocyte apoptosis, dark^{V} conferred striking hypermorphic gene activity without detectable effects upon steady-state expression. These results are consistent with negative-feedback models whereby the action of the Dark protein may be directly repressed by effector caspases, thereby setting an apoptotic threshold in cells that are specified for death.

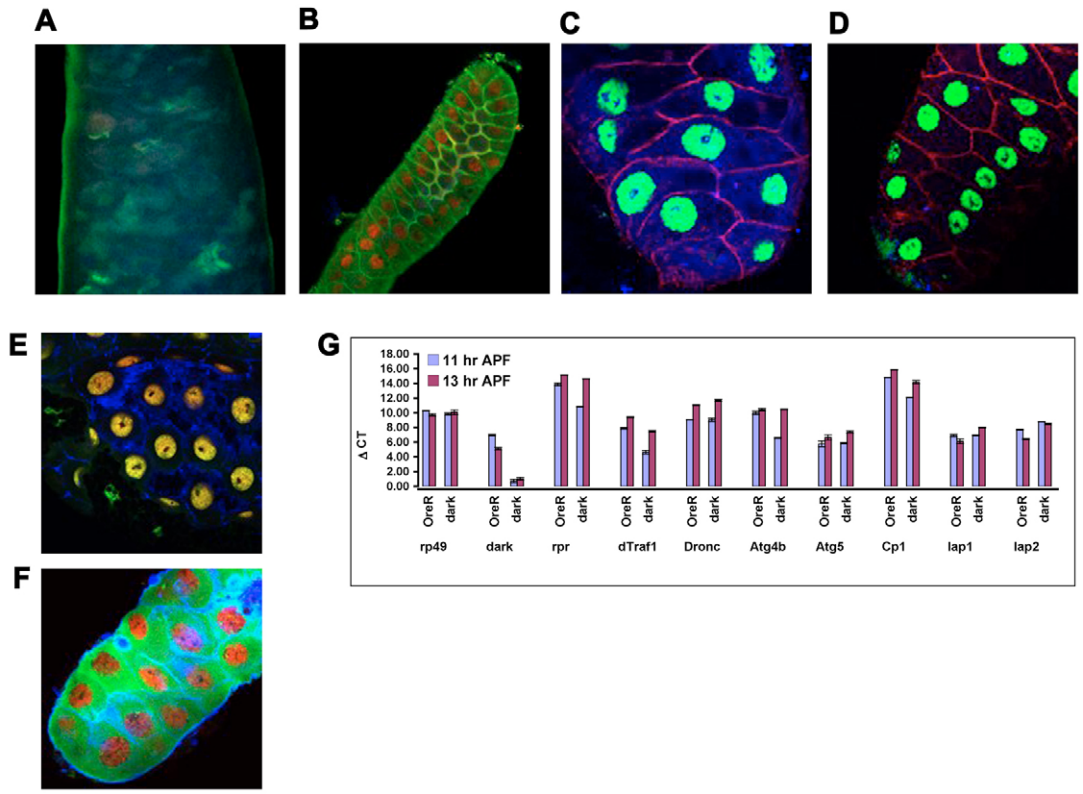

Fig. 4. *dark*^{82} salivary glands are defective for histolysis. (**A**,**B**) Confocal micrographs of salivary glands from wild-type (A) and dark^{82} (B) animals at 16 hours APF stained for a cytoplasmic protein, p127 (green), and a nuclear protein, BR-C (red). Head eversion, which marks the prepupal-pupal transition, has occurred in these animals. In wild type, larval salivary glands are completely histolysed, but in dark^{82} animals the glands persist and structural integrity is maintained. (**C**,**D**) Confocal micrographs showing immunohistochemical staining of salivary glands for anti-cleaved caspase 3 (blue), a marker for active DRICE (Yu et al., 2002), together with anti-actin, (red) and OliGreen, a nuclear stain (green). (C) Caspase activity (blue) in wild-type salivary glands is shown here at 12 hours APF, ~4 hours before final histolysis. (D) Caspase activity is starkly reduced in salivary glands of dark^{82} animals, shown here at 16 hours APF. (**E-G**) Ecdysone signaling and expression of death-related genes are unperturbed in *dark* mutant salivary glands. Immunohistochemical staining (E,F) shows nuclear accumulation of ecdysone-responsive transcription factors in persisting *dark* salivary glands at 16 hours APF. The confocal image in E shows coincident nuclear accumulation of Ecdysone Receptor (EcR, red) and BFTZ-F1 (green), counterstained for actin (blue). Overlapping stains for EcR and BFTZ-F1 produces a robust yellow signal in gland cell nuclei. In F, nuclear accumulation of E74A (red) is shown, with counterstaining for actin (blue) and the cytoplasmic protein Rab11 (green). (G) Pre-death expression profiles for the genes indicated were determined using real-time quantitative RT-PCR on RNA prepared from salivary glands dissected from wild-type (OreR) and dark^{82} animals at 11 hours and 13 hours APF (normalized from 18°C). The gene set analyzed here is a surrogate for profiles of pre-histolytic gene expression (Gorski et al., 2003). Expression levels are represented by ΔC_t values, where $\Delta C_t = C_t$ of no template control (set at 38 PCR cycles) – C_t of sample. C_t, or threshold cycle, is the PCR cycle at which a statistically significant increase in fluorescent signal can be detected above background. *Drosophila* rp49, used here as a control, showed no significant differences in expression. *dark* transcripts were not detected in mutant salivary glands, but, in all other respects, profiles between wild-type and dark glands were highly comparable.

Elimination of *dark* prevents salivary gland histolysis

To determine whether *dark* might function in autophagic cell death, we examined larval salivary glands, which normally histolyse at 16 hours after puparium formation (APF), manifesting vesicular features that are morphologically distinct from apoptosis (see Fig. 4A, Fig. 5A) (Lee and Baehrecke, 2001; Thummel, 2001). In *dark* mutants, these organs did not histolyse and, instead, persisted intact, even in 36-hour APF animals (Fig. 4B). Wild-type and *dark* glands were also stained for immunoreactivity with anti-cleaved caspase 3, an antibody that detects effector caspase activity in *Drosophila* tissues (Yu et al., 2002). In early pupariation stages (4 and 8 hours APF), wild-type salivary glands show little or no immunoreactivity (data not shown), but, four hours later (12 hours APF), widespread staining with anti-cleaved caspase 3 can be observed in the cytoplasm of these cells (Fig. 4C). By contrast, levels of anti-cleaved caspase 3 staining in *dark*$^{-}$ glands were starkly attenuated for reactivity at comparable stages and later (Fig. 4D).

These defects could reflect specific functional requirements for *dark* in histolysis or, alternatively, could result from a more generalized arrest in prepupal development. We can exclude the latter possibility, as persisting glands were always sampled from animals that had passed through the ‘head eversion stage’ into pupation (Ashburner, 1989) and numerous associated landmarks also proceeded on schedule (see below). Like many changes that occur during metamorphosis, salivary gland histolysis is tightly controlled by ecdysone and, hence, failure to histolyse might formally derive from a disruption of this hormonal axis (Yin and Thummel, 2005). To address this possibility, we examined

ecdysone-dependent signaling events known to occur during the period from 3 to 9 hours prior to histolysis (7-13 hours APF). For example, without *dark* function, ecdysone receptor (EcR) and other regulatory factors, such as BFTZ-f1 (Fig. 4E), E74A (Fig. 4F) and *Kruppel homolog* (not shown), accumulated in the nucleus of salivary gland cells. Likewise, in a survey of transcripts that anticipate salivary gland histolysis (Gorski et al., 2003; Lee et al., 2003), gene expression profiles from wild-type and $dark^{82}$ glands were highly comparable (see Fig. 4G). As an indicator of developmental progression, equivalent expression profiles (Fig. 4G) offer considerable statistical power, as a bulk analysis of 20-30 pairs of glands is represented at each time point. Therefore, by each criterion examined, hormonal signaling and associated target responses were unperturbed in *dark* animals. Together, these observations establish a specific requirement for the action of *dark* in salivary gland cell death and exclude generalized arrest or developmental delay as an explanation for defective histolysis.

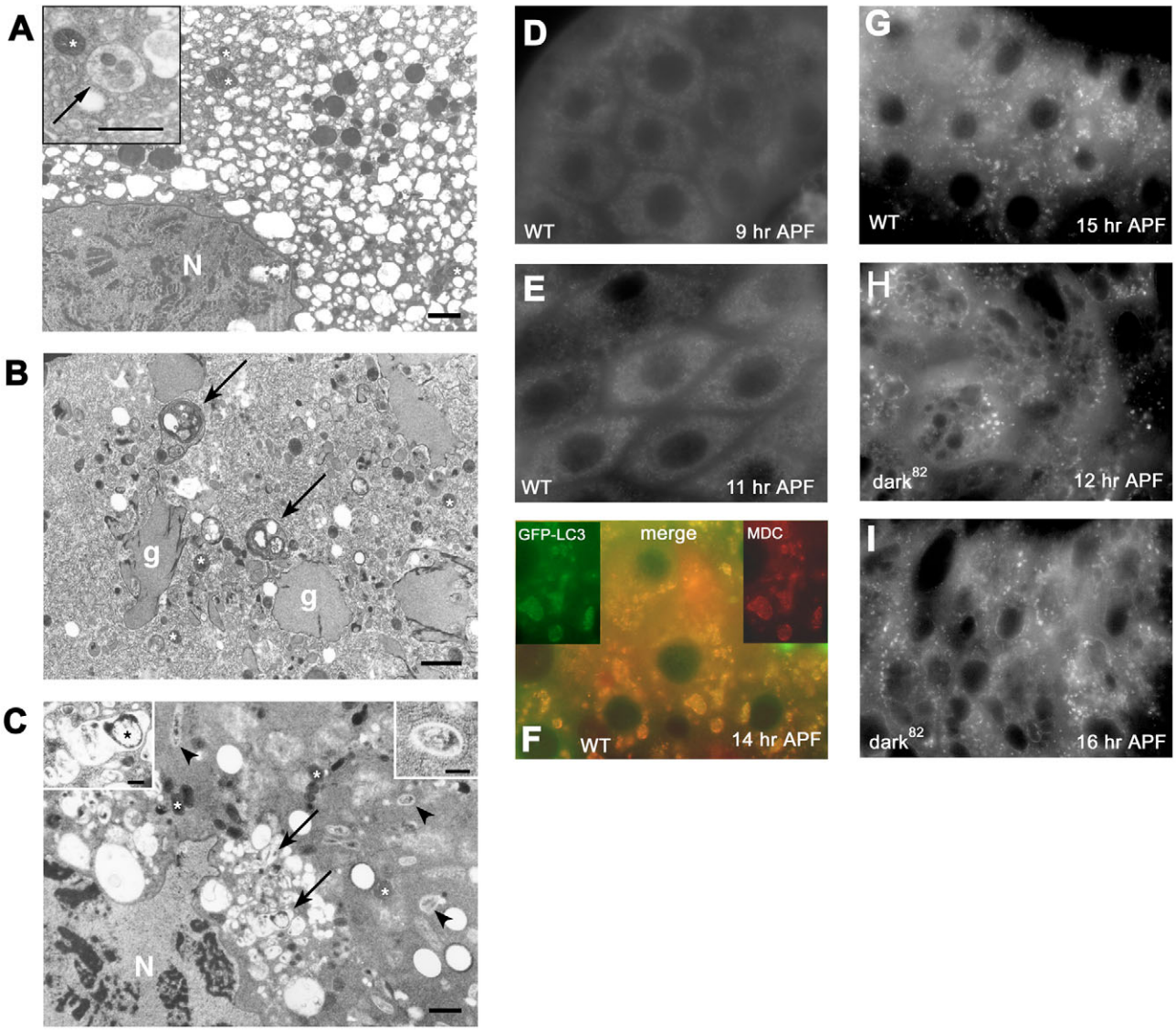

Fig. 5. Autophagy proceeds normally in *dark* mutant salivary glands. (**A-C**) Transmission EM of salivary gland cells. (A) A cytoplasm saturated with small vesicles and an electron dense nucleus (N) are indicative of ongoing cell death in wild-type cells at 14 hours APF. By contrast, salivary gland cells appear healthy in 14-hour APF $dark^{82}$ (B) and 24-hour APF $dark^{82}$ (C), showing no sign of cell death (compare the appearance of the nucleus in C with the nucleus in A). Arrows indicate autolysosomes in A-C, demonstrating that *dark* is not required for autophagy. Insets in panel C show enlargements of representative autophagosomes (top right corner) and autolysosomes (top left corner) seen in mutant glands. N, nucleus; g, secretory granule; asterisks indicate mitochondria. Scale bars: 1 μm; 250 nm for the insets. Arrowheads in C indicate autophagosomes. (**D-I**) Salivary glands dissected at the indicated time points (25°C) and stained with the acidic marker monodansylcadaverine (MDC) to detect autolysosomes (Munafo and Colombo, 2001). F shows a merged image of MDC staining (red) and detection of GFP-LC3 (green) (Rusten et al., 2004), a transgenic GFP marker for autophagosomes and autolysosomes in wild-type salivary glands (14 hours APF). At this stage, prior to histolysis, the overlap between MDC and GFP-LC3 is extensive, indicating an abundance of autolysosomes. (D-G) Time course of MDC staining in wild-type salivary glands. (D) At 9 hours APF, MDC staining is barely detectable. (E) At 11 hours APF, some punctate MDC-positive staining can be observed. However, by 14 hours APF (F) and in 15-hour APF glands (G), large MDC-positive structures are very conspicuous. Likewise, in comparably staged mutant glands, prominent MDC-positive vesicles are seen, shown here at 12 hours APF (H) and in persisting salivary glands 4 hours later (I).

Stimulation of autophagy occurs normally in persisting *dark* glands

We performed a series of histological and ultrastructural studies of mutant glands, with the goal of determining how *dark* might function in the histolysis of this organ. Two hours prior to histolysis of wild-type glands, the nucleus becomes electron dense, polytene chromosomes lose definition, vesicles saturate the cytoplasm and autolysosomes are prominent (Fig. 5A) (Farkas and Sutakova, 1998; Jiang et al., 1997; Juhasz and Sass, 2005). By stark contrast, comparably aged *dark* glands show no signs of vesicular saturation (Fig. 5B). Similarly, pre-histolytic changes that otherwise occur in the nucleus are not seen (Fig. 5C) and, instead, features characteristic of earlier-staged nuclei are retained. Like wild-type counterparts, however, numerous autolysosomes were evident in *dark* glands (Fig. 5B,C), indicating that *dark* function is not required for autophagy per se. To extend this analysis, we confirmed that monodansylcadaverine (MDC), an acidic marker that detects autolysosomes (Munafo and Colombo, 2001), overlapped with the signal derived from GFP-LC3 (Rusten et al., 2004), a transgenic marker of autophagy (Fig. 5F). Next, we established that, in wild-type salivary glands, dramatic accumulation of MDC staining anticipates PCD several hours prior to overt histolysis (Fig. 5D-G). We applied this methodology in *dark* animals and, likewise, observed a comparable abundance of MDC-stained structures in mutant glands (Fig. 5H,I), indicating that stimulation of autophagy, which normally anticipates histolysis, is not dependent on *dark* activity. Therefore, in this tissue, the action of *dark* in histolysis functions downstream of, or parallel to, an autophagic program.

DISCUSSION

Here, we show that *dark* encodes generalized functions in PCD. Loss of maternal and zygotic product caused profound defects, abolishing nearly all apoptotic deaths in the embryo. Likewise, elimination of zygotic *dark* prevented the histolytic death of salivary gland cells and also reversed drug-induced killing of hemocytes. These results establish widespread functions for *dark* in distinct models of programmed and stress-induced cell death. Moreover, because both apoptotic and histolytic forms of cell death were affected, it is clear that common effector pathways regulated by the apoptosome can specify apoptotic and non-apoptotic forms of PCD. The role for *dark* in PCD is not absolute, however, as rare apoptotic cell deaths were observed in animals lacking both the maternal and zygotic product. Although reminiscent of phenotypes associated with complete deletions in the *Reaper* region, loss of *dark* did not appear to perfectly phenocopy these, as occasional apoptotic cell deaths were observed. To substantiate this idea, we carefully compared the incidence of *dark*-independent cell deaths to the rare cell deaths that occur in H99 homozygous embryos. Among animals lacking both maternal and zygotic *dark*, an average of 8.9±2.0 cell deaths were found in late embryonic stages. However, only 3.1±2.1 cell deaths were found in comparably staged H99 embryos. Hence, in this respect, animals devoid of *dark* emulate cell death defects seen in animals lacking *dronc* (Xu et al., 2005). Together, these observations establish that, for a small population of embryonic cells, apoptotic activators in the *reaper* region can specify apoptosis without engaging the fly apoptosome. Similar pathways might occur in post-embryonic stages, but we caution against deriving firm conclusions in unaffected larval tissues, given the caveats relating to perdurance of maternally derived product.

Unlike its counterparts in the worm or the mouse, genetic elimination of *dark* produced a strictly lethal phenotype. Because ubiquitous and 'driver-specific' expression of a *dark* transgene complemented this phenotype, it was possible to map the focus of genetic activity responsible for restoring viability. We found that $dark^{82}$ lethality was reversed when expression was restored to cells of the post-embryonic CNS, but that complementation failed if *dark* was restored to hemocytes or imaginal discs. These results highlight essential functions for zygotic *dark* in the post-embryonic CNS and suggest that the action of this gene within other tissues may not be necessary for viability. Transgenic complementation also proved to be an effective means for distinguishing the wild-type gene action from that of derivatives with altered activities. By this approach, we determined that $dark^{v}$ encodes striking hypermorphic activity without affecting transgenic expression levels. As $dark^{v}$ is mutated at a caspase cleavage site (Fig. 3A-D), the data are consistent with negative-feedback models whereby the action of Dark is directly repressed by effector caspases, perhaps setting an apoptotic threshold in cells that are specified to die. These findings describe the first hypermorphic point mutation among all known alleles in the ced-4/Apaf1 gene family, and raise intriguing possibilities for investigating how life histories and stress responses might be impacted in adults with excessive apoptosomal activity. It is worth noting that, unlike cultured cell models, where full-length *dark* exhibits mild killing activity (Rodriguez et al., 1999), we found no evidence of dominant phenotypes associated with the forced overexpression of either the wild-type or the variant transgenes in tissues presented here (Fig. 3), or in other tissues, such as the eye (not shown). The different effects seen in culture cells versus transgenic animals might reflect authentic context-specific variance, or, alternatively, there may be a mild killing activity that does not manifest as a gross phenotype in the animal. Nevertheless, at least for most tissues and cells, it is unlikely that the levels of *Dark* protein alone qualify as a determinant of apoptosome activity. This inference, together with studies that exclude a fundamental requirement for *Drosophila* cytochrome c in formation of the apoptosome (Yu et al., 2005) or in models of apoptosis (Dorstyn et al., 2004; Zimmermann et al., 2002), suggests that, to function properly, *Dark* must be activated through an unknown mechanism.

Regression of *Drosophila* salivary glands in pupal development is a classic model of histolytic cell death, and dying cells in this gland appear morphologically distinct from cells undergoing apoptosis, indicating that novel cell death pathways may control forms of histolytic cell death (reviewed by Thummel, 2001). We assessed morphological, ultrastructural and molecular indicators to establish that, without *dark*, developmental progression was unperturbed, histolytic regression of this organ failed and salivary gland cells remained morphologically intact. Our results clearly establish a requisite function for Dark in the histolysis of salivary gland cells, despite the fact that PCD of these cells appears dissimilar from classical apoptosis. These observations are consistent with effects produced by p35, a broad-spectrum caspase inhibitor (Jiang et al., 1997; Lee and Baehrecke, 2001; Martin and Baehrecke, 2004), and with animals mutated for the apical caspase *dronc* (Daish et al., 2004). Because apoptotic and histolytic forms of cell death are similarly impacted by the same mutation, we conclude that common effector pathways, regulated by the apoptosome, underlie morphologically distinct forms of PCD.

The induction of autophagy that anticipates salivary gland histolysis may act as part of a novel killing mechanism in these cells (Lee and Baehrecke, 2001; Myohara, 2004; Thummel, 2001), and in mammalian cell death models as well (Shimizu et al., 2004; Yu et

al., 2004). However, in other circumstances, 'self-digestion' clearly promotes survival when apoptosis in prevented (Lum et al., 2005), and, consequently, it is important to understand how links between autophagy and cell death may instruct cell fates (Levine and Klionsky, 2004). As *dark*^{82} organs do not regress like their wild-type counterparts, *dark*^{82} animals afford a unique opportunity to dissect the relationship between histolysis and autophagy. Because the stimulation of autophagy continued in glands that failed to histolyse, we suggest that induced autophagy per se is not the 'lethal event' mediating histolysis of this organ. Instead, the epistasis experiments described here demonstrate that the induction of autophagy lies upstream of, or parallel to, the apoptosome in this model of histolytic cell death.

We gratefully acknowledge support to J.M.A. from the NIH (GM072124), and VEGA (2/3025/23) and APVT (51-027402) grants to R.F., and an NKFP grant (1/a/005/04) to M.S. We are also grateful to Kathleen Galindo for germ line transformations, to T. E. Rusten and H. Stenmark for GFP-LC3 flies, and to Margaret Hickson for administrative support.

References

Abrams, J. M. (1999). An emerging blueprint for apoptosis in Drosophila. *Trends Cell Biol.* **9**, 435-440.
Abrams, J. M., White, K., Fessler, L. and Steller, H. (1993). Programmed cell death during *Drosophila* embryogenesis. *Development* **117**, 29-44.
Adrain, C., Slee, E. A., Harte, M. T. and Martin, S. J. (1999). Regulation of apoptotic protease activating factor-1 oligomerization and apoptosis by the WD-40 repeat region. *J. Biol. Chem.* **274**, 20855-20860.
Ashburner, M. (1989). *Drosophila: A Laboratory Handbook*. Cold Spring Harbor: Cold Spring Harbor Laboratory Press.
Chai, J., Yan, N., Huh, J. R., Wu, J. W., Li, W., Hay, B. A. and Shi, Y. (2003). Molecular mechanism of Reaper-Grim-Hid-mediated suppression of DIAP1-dependent Dronc ubiquitination. *Nat. Struct. Biol.* **10**, 892-898.
Chew, S. K., Akdemir, F., Chen, P., Lu, W. J., Mills, K., Daish, T., Kumar, S., Rodriguez, A. and Abrams, J. M. (2004). The apical caspase dronc governs programmed and unprogrammed cell death in Drosophila. *Dev. Cell* **7**, 897-907.
Chou, T. B. and Perrimon, N. (1996). The autosomal FLP-DFS technique for generating germline mosaics in Drosophila melanogaster. *Genetics* **144**, 1673-1679.
Christich, A., Kauppila, S., Chen, P., Sogame, N., Ho, S. I. and Abrams, J. M. (2002). The Damage-responsive drosophila gene sickle encodes a novel IAP binding protein similar to but distinct from reaper, grim, and hid. *Curr. Biol.* **12**, 137-140.
Daish, T. J., Mills, K. and Kumar, S. (2004). Drosophila caspase DRONC is required for specific developmental cell death pathways and stress-induced apoptosis. *Dev. Cell* **7**, 909-915.
Danial, N. N. and Korsmeyer, S. J. (2004). Cell death: critical control points. *Cell* **116**, 205-219.
Ditzel, M., Wilson, R., Tenev, T., Zachariou, A., Paul, A., Deas, E. and Meier, P. (2003). Degradation of DIAP1 by the N-end rule pathway is essential for regulating apoptosis. *Nat. Cell Biol.* **5**, 467-473.
Dorstyn, L., Mills, K., Lazebnik, Y. and Kumar, S. (2004). The two cytochrome c species, DC3 and DC4, are not required for caspase activation and apoptosis in Drosophila cells. *J. Cell Biol.* **167**, 405-410.
Drapeau, M. D., Radovic, A., Wittkopp, P. J. and Long, A. D. (2003). A gene necessary for normal male courtship, yellow, acts downstream of fruitless in the Drosophila melanogaster larval brain. *J. Neurobiol.* **55**, 53-72.
Farkas, R. and Sutakova, G. (1998). Ultrastructural changes of Drosophila larval and prepupal salivary glands cultured in vitro with ecdysone. *In Vitro Cell. Dev. Biol. Anim.* **34**, 813-823.
Farkas, R. and Mechler, B. M. (2000). The timing of drosophila salivary gland apoptosis displays an l(2)gl-dose response. *Cell Death Differ.* **7**, 89-101.
Geisbrecht, E. R. and Montell, D. J. (2004). A role for Drosophila IAP1-mediated caspase inhibition in Rac-dependent cell migration. *Cell* **118**, 111-125.
Gorski, S. M., Chittaranjan, S., Pleasance, E. D., Freeman, J. D., Anderson, C. L., Varhol, R. J., Coughlin, S. M., Zuyderduyn, S. D., Jones, S. J. and Marra, M. A. (2003). A SAGE approach to discovery of genes involved in autophagic cell death. *Curr. Biol.* **13**, 358-363.
Goto, A., Kadowaki, T. and Kitagawa, Y. (2003). Drosophila hemolectin gene is expressed in embryonic and larval hemocytes and its knock down causes bleeding defects. *Dev. Biol.* **264**, 582-591.
Goyal, L. (2001). Cell death inhibition: keeping caspases in check. *Cell* **104**, 805-808.
Grether, M. E., Abrams, J. M., Agapite, J., White, K. and Steller, H. (1995). The *head involution defective* gene of *Drosophila melanogaster* functions in programmed cell death. *Genes Dev.* **9**, 1694-1708.
Gustafson, K. and Boulianne, G. L. (1996). Distinct expression patterns detected within individual tissues by the GAL4 enhancer trap technique. *Genome* **39**, 174-182.
Hays, R., Wickline, L. and Cagan, R. (2002). Morgue mediates apoptosis in the Drosophila melanogaster retina by promoting degradation of DIAP1. *Nat. Cell Biol.* **4**, 425-431.
Hrdlicka, L., Gibson, M., Kiger, A., Micchelli, C., Schober, M., Schock, F. and Perrimon, N. (2002). Analysis of twenty-four Gal4 lines in Drosophila melanogaster. *Genesis* **34**, 51-57.
Hu, Y. M., Ding, L. Y., Spencer, D. M. and Nunez, G. (1998). WD-40 repeat region regulates Apaf-1 self-association and procaspase-9 activation. *J. Biol. Chem.* **273**, 33489-33494.
Jiang, C., Baehrecke, E. H. and Thummel, C. S. (1997). Steroid regulated programmed cell death during Drosophila metamorphosis. *Development* **124**, 4673-4683.
Juhasz, G. and Sass, M. (2005). Hid can induce, but is not required for autophagy in polyploid larval Drosophila tissues. *Eur. J. Cell Biol.* **84**, 491-502.
Kanuka, H., Sawamoto, K., Inohara, N., Matsuno, K., Okano, H. and Miura, M. (1999). Control of the cell death pathway by Dapaf-1, a Drosophila Apaf-1/CED-4-related caspase activator. *Mol. Cell* **4**, 757-769.
Lee, C. Y. and Baehrecke, E. H. (2001). Steroid regulation of autophagic programmed cell death during development. *Development* **128**, 1443-1455.
Lee, C. Y., Clough, E. A., Yellon, P., Teslovich, T. M., Stephan, D. A. and Baehrecke, E. H. (2003). Genome-wide analyses of steroid- and radiation-triggered programmed cell death in Drosophila. *Curr. Biol.* **13**, 350-357.
Levine, B. and Klionsky, D. J. (2004). Development by self-digestion: molecular mechanisms and biological functions of autophagy. *Dev. Cell* **6**, 463-477.
Li, L., Thomas, R. M., Suzuki, H., De Brabander, J. K., Wang, X. and Harran, P. G. (2004). A small molecule Smac mimic potentiates TRAIL- and TNFalpha-mediated cell death. *Science* **305**, 1471-1474.
Lum, J. J., Bauer, D. E., Kong, M., Harris, M. H., Li, C., Lindsten, T. and Thompson, C. B. (2005). Growth factor regulation of autophagy and cell survival in the absence of apoptosis. *Cell* **120**, 237-248.
Manseau, L., Baradaran, A., Brower, D., Budhu, A., Elefant, F., Phan, H., Philp, A. V., Yang, M., Glover, D., Kaiser, K. et al. (1997). GAL4 enhancer traps expressed in the embryo, larval brain, imaginal discs, and ovary of Drosophila. *Dev. Dyn.* **209**, 310-322.
Martin, D. N. and Baehrecke, E. H. (2004). Caspases function in autophagic programmed cell death in Drosophila. *Development* **131**, 275-284.
Martin, S. J. (2002). Destabilizing influences in apoptosis. Sowing the seeds of IAP destruction. *Cell* **109**, 793-796.
Meier, P., Silke, J., Leevers, S. J. and Evan, G. I. (2000). The Drosophila caspase DRONC is regulated by DIAP1. *EMBO J.* **19**, 598-611.
Mills, K., Daish, T. and Kumar, S. (2005). The function of the Drosophila caspase DRONC in cell death and development. *Cell Cycle* **4**, 744-746.
Moriishi, K., Huang, D. C. S., Cory, S. and Adams, J. M. (1999). Bcl-2 family members do not inhibit apoptosis by binding the caspase activator Apaf-1. *Proc. Natl. Acad. Sci. USA* **96**, 9683-9688.
Munafo, D. B. and Colombo, M. I. (2001). A novel assay to study autophagy: regulation of autophagosome vacuole size by amino acid deprivation. *J. Cell Sci.* **114**, 3619-3629.
Myohara, M. (2004). Real-time observation of autophagic programmed cell death of Drosophila salivary glands in vitro. *Dev. Genes Evol.* **214**, 99-104.
Park, M., Wu, X., Golden, K., Axelrod, J. D. and Bodmer, R. (1996). The wingless signaling pathway is directly involved in Drosophila heart development. *Dev. Biol.* **177**, 104-116.
Rodriguez, A., Oliver, H., Zou, H., Chen, P., Wang, X. D. and Abrams, J. M. (1999). Dark is a Drosophila homologue of Apaf-1/CED-4 and functions in an evolutionarily conserved death pathway. *Nat. Cell Biol.* **1**, 272-279.
Rusten, T. E., Lindmo, K., Juhasz, G., Sass, M., Seglen, P. O., Brech, A. and Stenmark, H. (2004). Programmed autophagy in the Drosophila fat body is induced by ecdysone through regulation of the PI3K pathway. *Dev. Cell* **7**, 179-192.
Ryoo, H. D., Bergmann, A., Gonen, H., Ciechanover, A. and Steller, H. (2002). Regulation of Drosophila IAP1 degradation and apoptosis by reaper and ubcD1. *Nat. Cell Biol.* **4**, 432-438.
Salvesen, G. S. and Abrams, J. M. (2004). Caspase activation–stepping on the gas or releasing the brakes? Lessons from humans and flies. *Oncogene* **23**, 2774-2784.
Shimizu, S., Kanaseki, T., Mizushima, N., Mizuta, T., Arakawa-Kobayashi, S., Thompson, C. B. and Tsujimoto, Y. (2004). Role of Bcl-2 family proteins in a non-apoptotic programmed cell death dependent on autophagy genes. *Nat. Cell Biol.* **6**, 1221-1228.
Silke, J. H., Kratina, T., Ekert, P. G., Pakusch, M. and Vaux, D. L. (2004). Unlike Diablo/smac, grim promotes global ubiquitination and specific degradation of XIAP and neither cause apoptosis. *J. Biol. Chem.* **279**, 4313-4321.
Spierings, D., McStay, G., Saleh, M., Bender, C., Chipuk, J., Maurer, U. and Green, D. R. (2005). Connected to death: the (unexpurgated) mitochondrial pathway of apoptosis. *Science* **310**, 66-67.

Thummel, C. S. (2001). Steroid-triggered death by autophagy. *BioEssays* **23**, 677-682.
Wang, S. L., Hawkins, C. J., Yoo, S. J., Muller, H. A. J. and Hay, B. A. (1999). The Drosophila caspase inhibitor DIAP1 is essential for cell survival and is negatively regulated by HID. *Cell* **98**, 453-463.
White, K., Grether, M., Abrams, J. M., Young, L., Farrell, K. and Steller, H. (1994). Genetic control of programmed cell death in *Drosophila*. *Science* **264**, 677-683.
Wilson, R., Goyal, L., Ditzel, M., Zachariou, A., Baker, D. A., Agapite, J., Steller, H. and Meier, P. (2002). The DIAP1 RING finger mediates ubiquitination of Dronc and is indispensable for regulating apoptosis. *Nat. Cell Biol.* **4**, 445-450.
Wing, J. P., Schwartz, L. M. and Nambu, J. R. (2001). The RHG motifs of Drosophila Reaper and Grim are important for their distinct cell death-inducing abilities. *Mech. Dev.* **102**, 193-203.
Wing, J. P., Karres, J. S., Ogdahl, J. L., Zhou, L., Schwartz, L. M. and Nambu, J. R. (2002a). Drosophila sickle is a novel grim-reaper cell death activator. *Curr. Biol.* **12**, 131-135.
Wing, J. P., Schreader, B. A., Yokokura, T., Wang, Y., Andrews, P. S., Huseinovic, N., Dong, C. K., Ogdahl, J. L., Schwartz, L. M., White, K. et al. (2002b). Drosophila Morgue is an F box/ubiquitin conjugase domain protein important for grim-reaper mediated apoptosis. *Nat. Cell Biol.* **4**, 451-456.
Wu, J. W., Cocina, A. E., Chai, J. J., Hay, B. A. and Shi, Y. G. (2001). Structural analysis of a functional DIAP1 fragment bound to grim and hid peptides. *Mol. Cell* **8**, 95-104.
Xu, D., Li, Y., Arcaro, M., Lackey, M. and Bergmann, A. (2005). The CARD-carrying caspase Dronc is essential for most, but not all, developmental cell death in Drosophila. *Development* **132**, 2125-2134.
Yin, V. P. and Thummel, C. S. (2005). Mechanisms of steroid-triggered programmed cell death in Drosophila. *Semin. Cell Dev. Biol.* **16**, 237-243.
Yoo, S. J., Huh, J. R., Muro, I., Yu, H., Wang, L., Wang, S. L., Feldman, R. M., Clem, R. J., Muller, H. A. and Hay, B. A. (2002). Hid, Rpr and Grim negatively regulate DIAP1 levels through distinct mechanisms. *Nat. Cell Biol.* **4**, 416-424.
Yu, L., Alva, A., Su, H., Dutt, P., Freundt, E., Welsh, S., Baehrecke, E. H. and Lenardo, M. J. (2004). Regulation of an ATG7-beclin 1 program of autophagic cell death by caspase-8. *Science* **304**, 1500-1502.
Yu, S. Y., Yoo, S. J., Yang, L., Zapata, C., Srinivasan, A., Hay, B. A. and Baker, N. E. (2002). A pathway of signals regulating effector and initiator caspases in the developing Drosophila eye. *Development* **129**, 3269-3278.
Yu, X., Wang, L., Acehan, D., Wang, X. and Akey, C. W. (2005). Three-dimensional structure of a double apoptosome formed by the Drosophila Apaf-1 related killer. *J. Mol. Biol.* **355**, 577-589.
Zachariou, A., Tenev, T., Goyal, L., Agapite, J., Steller, H. and Meier, P. (2003). IAP-antagonists exhibit non-redundant modes of action through differential DIAP1 binding. *EMBO J.* **22**, 6642-6652.
Zhou, L., Song, Z. W., Tittel, J. and Steller, H. (1999). HAC-1, a Drosophila homolog of APAF-1 and CED-4 functions in developmental and radiation-induced apoptosis. *Mol. Cell* **4**, 745-755.
Zimmermann, K. C., Ricci, J. E., Droin, N. M. and Green, D. R. (2002). The role of ARK in stress-induced apoptosis in Drosophila cells. *J. Cell Biol.* **156**, 1077-1087.